Open-source tool-box for identifying envelope dynamics of detached residential buildings

Elias N. PERGANTIS[1*], Jaewon PARK[1], Trevor J. BIRD[1], PRIYADARSHAN[1], Davide ZIVIANI[1], Kevin J. KIRCHER[1*]

[1]Ray W. Herrick Laboratories, School of Mechanical Engineering, Purdue University
West Lafayette, 47907-2099, USA

*Corresponding Author: epergant@purdue.edu, kircher@purdue.edu

ABSTRACT

The rapid electrification of residential buildings has created rising concerns about the ability of the power grid to deal with seasonal electric space conditioning peaks. Better control of home heating and cooling systems can help solve this problem. However, unlike other control areas where extensive data are often available, each home presents a unique plant for which data are limited. This complicates the development of advanced control systems. This paper presents an open-source toolbox that researchers and industry can use as a plug-and-play tool for identifying the thermal dynamics of detached single-family homes. The tool supports identification of 3R2C and 2R1C thermal circuit models and can be trained using either thermal or electrical data alongside temperature measurements. The 2R1C method uses a computationally inexpensive constrained least squares formulation, while the 3R2C used a meta-heuristic genetic algorithm. The thermal mass temperature is treated as a hidden state with a Kalman Filter in place. The system is tested on a real-world building for prediction accuracy of indoor temperature and heat supply. In these tests, the root-mean-square hour-ahead temperature prediction errors are 0.8 ℃ and 0.57 ℃ for the 2R1C and 3R2C models, respectively. Under highly transient indoor conditions, such as fast indoor temperature set-point changes, the 3R2C performs better, while under more steady conditions the two model structures perform similarly.

1. DIFFERENT METHODS OF MODEL IDENTIFICATION FOR BUILDINGS

The residential sector is responsible for greater than 20 % of U.S. CO2 emissions, 20 % of the energy consumption, and 40 % of total electricity use, in 2020 alone, residential buildings in the U.S. consumed nearly 21 quadrillion BTUs of primary energy, of which space conditioning (heating and cooling) and water heating accounted for approximately 56% (EIA 2021). Increased efforts to promote electrification create tremendous opportunities for efficiency improvements while also great challenges for grid reliability and robustness (González-Torres et al. 2022). Optimal controls can significantly aid in this effort, however, the paradigm of the simple P, PI, or on-off thermostat has not changed in almost 60 years. As such, simulation based optimal controls have become a trendy research field, with countless simulation-based optimal controls of building studies (MPC, or otherwise) being written every year (Drgona et al. 2020, Zhang et al. 2022). One could categorize optimal studies based on the model used, whether black-box, grey-box, or white-box. White-box models usually involve creating an EnergyPlus model of the building at hand, after which, some model reduction technique can be used to generate a lower-order RC model. Similarly, most often than not, grey-box or black-box based models also involve the incorporation of some white-box model, either for the generation of training sets (black-box) or to model internal and solar gains (grey-box) (Khabbazi et al. 2024). Although these methods are acceptable for commercial buildings, where information on material properties and detailed engineering schematics (floor plan, zoning, etc.) are readily available, for residential buildings, they can result in poor performance (Dong and Lam 2013, Kim et al. 2022). Therefore, for the optimal control of residential building methods that can obtain a model from limited data are to be preferred. Black-box approaches face a significant limitation in this front due to low data availability as well as white-box models due to their need for extensive building specific information. In this work, a novel method is presented whereupon low-order building grey-box models can be trained using limited sensor data by combining parameter estimation methods (regression, multiparameter optimization, GA) with the thermal powers arising from unknown thermal gains from occupants, devices, envelope non-linearities, heat pump non-linearities, etc. being obtained from a Support Vector Machine (SVM). Although the potential of grey-box methods for training with smaller datasets is widely known, limited open-source resources exist for training RC models

(Drgona et al. 2020, Connick and Helsen 2016, Blum et al. 2019, Pergantis et al. 2024), especially in the cases that white-box models can not be utilized to aid in generating synthetic internal gains data. Especially for detached residential buildings were building parameters are often unknown, simple easy to implement identification algorithms will be paramount in the penetration of smart control algorithm.

This paper is organized as follows: firstly, two building envelope models are presented primarily aimed at detached residential buildings making 64% of the US residential stock (US Census 2019); a lower order, and a higher-order with hidden states (state-of-the-art), they are trained using real building data, then these models are compared for a practical application in a residential building. The dataset and codes to train these models are made publicly available for other researchers to test and improve. The tools provided in this paper can be found in Pergantis 2024 . A full user guide is provided in the relevant repository, with future plans to move the codes from MATLAB to Python for a fully open-source version.

2. MODEL STRUCTURES

2.1 Two-resistance one-capacitance model

The vast majority of residential buildings in the US are detached single family homes stock (US Census 2019). Homes are often built out of wood, which has a large thermal resistance but a far lower thermal capacitance. A simple 1st order differential equation can be derived for the net air temperature in the house (T) in the form of Eq. 1 where it is assumed that heat transfer does not occur between the thermal mass (internal, T_m) of the building, and the ambient temperature (θ). The thermal capacitance related to the indoor air is C, while the resistance between the indoor mass and mixed indoor air is denoted by R_m and the ambient environment by R_{out}. The heat supply $\dot{Q}_c$ is provided by the heating/cooling equipment and $\dot{Q}_e$ represents the "exogenous heat supply", heat addition or subtraction that cannot be attributed to the heat supply method (heat pump, gas) in the physical building. The reader is referred to the nomenclature section for more information on units.

$$C\dot{T}(t) = \frac{T_m(t) - T(t)}{R_m} + \frac{\theta(t) - T(t)}{R_{out}} + \dot{Q}_c(t) + \dot{Q}_e(t) \tag{1}$$

In this resistance-capacitance formulation it is assumed that the internal mass acts as a node without any capacitance of its own, and that the physical parameters remain time invariant.

$$\begin{aligned} R &= \frac{R_m R_{out}}{R_m + R_{out}}; \theta_{eq} = \frac{R_{out} T_m + R_m \theta}{R_m + R_{out}} \\ C\dot{T}(t) &= \frac{\theta_{eq}(t) - T(t)}{R} + \dot{Q}_c(t) + \dot{Q}_e(t) \end{aligned} \tag{2}$$

This allows for the Eq. 1 to be reformulated in an equivalent 1R1C using the effective outdoor temperature (θ_{eq}) and thermal resistance R. Assuming a zero-order hold on the input signals with time step Δt (h), the continuous-time dynamics can be exactly discretized to:

$$T(k+1) = \alpha T(k) + (1-\alpha)\left[\theta(k) + R\left(\dot{Q}_c(k) + \dot{Q}_e(k)\right)\right] \tag{3}$$

where k indexes discrete time and α can be derived from the lump air analysis as:

$$\alpha = \exp\left(-\frac{\Delta T}{RC}\right) \tag{4}$$

2.2 Three-resistance two-capacitance model

Considering the thermal capacitance of the internal mass to be nonnegligible, another model, which has three thermal resistances and two capacitances, is developed. The thermal resistance is extended to include the energy transfer of the internal mass with indoor air and surroundings as shown in Fig. 1. The model formulation assumes the same linear-

time-invariant system dynamics as previously discussed. Since there are two thermal capacitances, the formulation is essentially two 1st order ODEs which are coupled, expressed in a state-space representation in following manner:

$$\dot{x}(t) = Ax(t) + Bu(t) + Wd(t);\ \ y(t) = [1 \quad 0]x(t);\ \ x = [T_{in} \quad T_m]^T \tag{5}$$

where the state vector includes two temperature states of indoor air and internal mass, respectively. The system matrix, *A*, input matrix, *B*, and disturbance matrix, *W*, are described in following expressions:

$$A = \begin{bmatrix} -\frac{1}{R_{out}C} - \frac{1}{R_mC} & \frac{1}{R_mC} \\ \frac{1}{R_mC_m} & -\frac{1}{R_mC_m} - \frac{1}{R_{m,out}C_m} \end{bmatrix};\ B = \begin{bmatrix} \frac{1}{R_{out}C} & \frac{1}{C} & \frac{A}{C} \\ \frac{1}{R_{out}C} & 0 & \frac{A_m}{C_m} \end{bmatrix};\ W = \begin{bmatrix} \frac{1}{C} & 0 \end{bmatrix}^T \tag{6}$$

The thermal resistances and capacitances are equivalent to those denoted in Fig. 1. Area terms, *A* and A_m, for indoor air and internal mass are used for the calculation of solar irradiation heat transfer. The input vector, *u(t)*, then consists of three different measurable aspects of heat transfer: outdoor air temperature, heat supply, and solar irradiation. In this study, surface solar radiation is used directly, and it is assumed window orientation, and other effects are captured in the training of the dynamic equations. Lastly, the disturbance, *d*, is the unknown heat supply to the system. It is equivalent to the exogenous heat supply term described in the previous section in its physical meaning although the numerical values do not necessarily match. It is assumed that this disturbance affects only the indoor air directly and not the thermal mass.

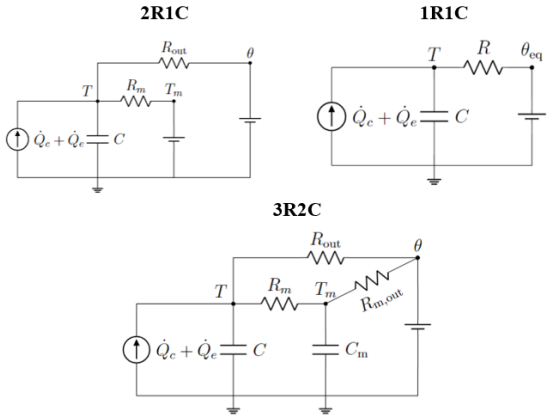

Figure 1: Thermal circuit model structures used in this work.

3. TEST SITE

3.1 Training data

The DC House is the first field test of this technique. It is a 3-bedroom 2-floor detached residential building, shown in Fig. 2. From the sensor infrastructure at the house designed with an aim of minimal installations and cost, the heat supply (input) and indoor return mixed air temperature (state) are available. Other inputs are obtained using a weather service (Oikolab) while the thermal mass of the building is treated as a hidden state.

Figure 2: This paper uses field data from a 1920s-era home that has been deeply retrofitted with insulation and all-electric appliances.

The exterior walls have foam insulation with an R-Value of 3.5 °C m^2/W. Code-minimum U-8 W/ m^2/°C windows make up about 20% of the exterior wall area. Since this is a cold climate (IECC 5A), the methodology in this work is focued on heating. In the cooling work of Pergantis et al. (2024), it is found that retraining of thermal parameters and internal gains is needed for the cooling dominated months.

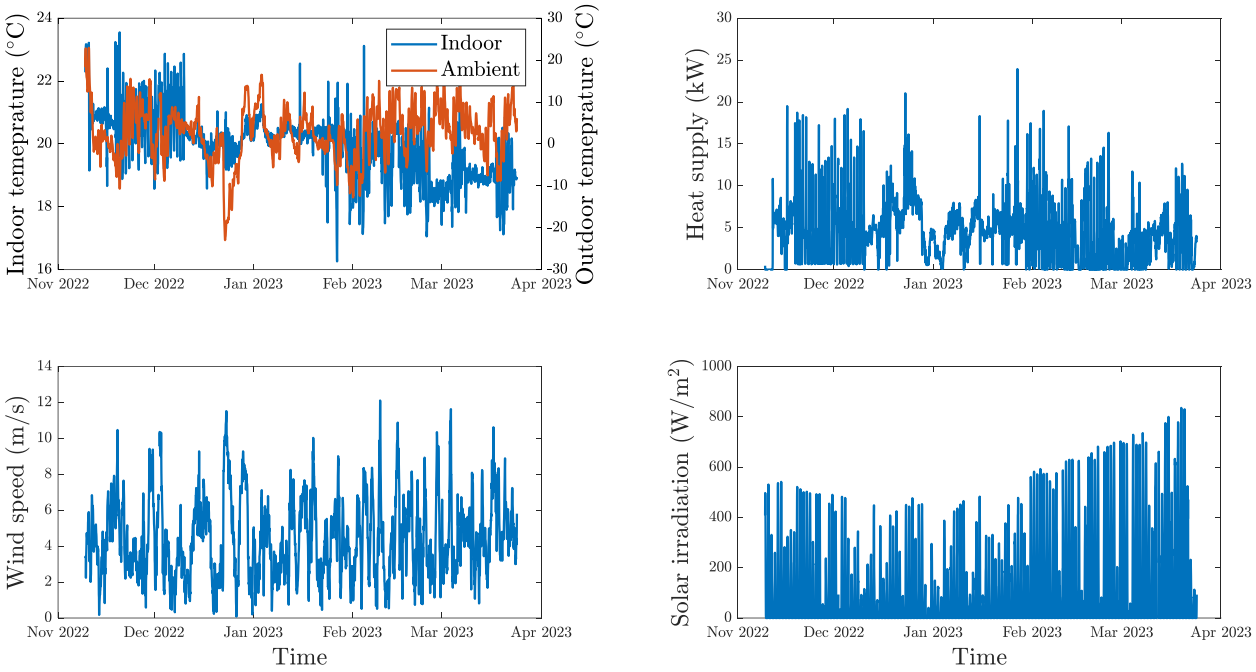

Figure 3: Local measurements (indoor temperature, heat supply) and weather service data (outdoor temperature, wind speed, solar irradiance) used to train thermal envelope models.

3.2 Sensing equipment

The sensing infrastructure used in this study is shown in Table 1. Sensor error have not been considered in this study, with error being lumped in the exogenous heat supply term. This is also true for the weather service temperature, where since there is no local weather station at the house, is also lumped in the exogenous disturbance. To smooth the error from the temperature thermocouple measurements, eight thermocouples are in place in the supply and return ducts, and the average of each ensemble is used to compute the temperature. The greatest source of uncertainty is the airflow sensor, which is prone to drift and accumulation of dust, due to its location before the filter. To account for this, systematic cleaning is performed as well as calibration with differential pressure and manufacturer fan curves.

Table 1: Temperature and air flow sensors.

Equipment/Sensor	Cost [USD $]	Purpose	Error (-)
Yokogawa GM 10 DAQ	1,800	Thermocouple DAQ (T-type)	0.5 (°C)
Ebtron GTx116- P+	600	Airflow sensor	5%

4. IDENTIFICATION PROCEDURE

4.1 Two-resistance one-capacitance model

The training of the 2R1C can be split into two separate sub-training processes. Firstly, if the indoor air temperature T is approximately constant and equal to T_m, and if the exogenous thermal power is approximately constant (nighttime period), Eq. 2 can be reduced to its steady state:

$$\begin{aligned} &T(t)-\theta(t) \approx R_{out}\left[\dot{Q}_c(t)+\dot{Q}_e(t)\right]=R_{out}\left[\dot{Q}_c(t)+\dot{Q}_e\right] \\ &y=X\beta, \text{ where: } y=\begin{bmatrix} T(t_1)-\theta(t_1) \\ \vdots \\ T(t_n)-\theta(t_n) \end{bmatrix} \\ &X=\begin{bmatrix} 1 & \dot{Q}_c(t_1) \\ \vdots & \vdots \\ 1 & \dot{Q}_c(t_n) \end{bmatrix} \text{ and } \beta=\begin{bmatrix} R_{out}\dot{Q}_e \\ R_{out} \end{bmatrix} \end{aligned} \tag{7}$$

where all that was done effectively is pose the identification problem as least squares (LS) by manipulating the original equations. The problem is further formulated as constrained LS. CVX (Grant and Boyd 2014) was used to solve the problem of minimizing the MSE so that the parameter vector, β, could be constrained for a physically plausible solution to exist ($\beta(1) < 9$ and $\beta(2) < 5$). Having computed R_{out} via deterministic least squares, R_m and C are missing, as well as T_m (hidden state). Since T_m is a continuous state, it has been assumed that T_m is constant and fixed at the sample mean of the indoor air temperature. Subsequently, using the discrete form of the ODE given in Eq. 3, is rearrange for the missing variables in Eq. 8:

$$\begin{aligned} &T(k+1)-\theta(k)-R\dot{Q}_c(k) \approx \alpha(T(k)-\theta(k)-R\dot{Q}_c(k))+v \\ &known=T,\dot{Q}_c,\theta;\ unknown=R,v,\alpha \\ &where\ v=(1-\alpha)R\dot{Q}_e \end{aligned} \tag{8}$$

The approximation arises from the assumption that the exogenous heat supply is constant, which is necessary for identification purposes. Eq. 8 forms another least squares problem. The solution procedure is outlined below:

- Assume R_m ε (0.1,10) [kW].
- Perform LS via equation 7 to identify α and v for varying R_m.
- Find the values of R_m^* that minimizes the weighted sum of the RMSE between the validation and training sets, weight = 0.2 was found to perform well.
- Use R_m^* to identify α and v (one last LS).

Finally, having trained the model, $\dot{Q}_e$ can be calculated directly for training purposes by re-arranging Eq. 3. as:

$$\dot{Q}_e(k)=\left[\frac{T(k+1)-\alpha T(k)}{(1-\alpha)}-\theta(k)\right]\frac{1}{R}-\dot{Q}_c(k) \tag{9}$$

Once the model is fully trained ($\dot{Q}_e$), one could calculate the thermal power using Eq. 10, simply by using setpoints or indoor temperatures:

$$\dot{Q}_c(k)=\left[\frac{T(k+1)-\alpha T(k)}{(1-\alpha)}-\theta(k)\right]\frac{1}{R}-\dot{Q}_e(k) \tag{10}$$

A critical issue with the current model was identified to lie what is known as "overfitting the temperature" where upon to reduce the error in the temperature prediction (Eq. 8) the model would overpredict the thermal capacitance of the building, which however results in high error to the power in Eq. 10. This trend is shown in Fig. 4. An RMSE (Heat Supply) < 3 kW was found to yield an error in energy (integral of power), of less than 15% which is acceptable for control purposes (Blum et al. 2019). As such, C = 6.5 kWh/°C was selected. The results of this process are summarized in Table 1. The time step ΔT = 1 h was used in this study.

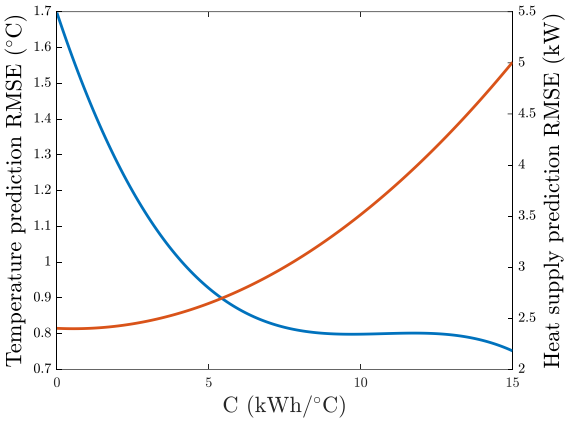

Figure 4: Joint fitting of thermal capacitance of the indoor air on heat supply and temperature (Δt = 1 hour). As the thermal capacitance increases, temperature prediction accuracy improves but heat supply predictions degrade.

TABLE I. TRAINED PHYSICAL PARAMETERS OF 2R1C MODEL

Time Step (Δt) [hours]	**Thermal Parameters**					
	R_m (*kWh/°C*)	R_{out} (*kWh/°C*)	R (*kWh/°C*)	T_m (*°C*)	C (*kWh/°C*)	C_{fix} (*kWh/°C*)
1	1.06	2.04	0.7	20.6	13.6	6.5
0.5	6.84	1.9	1.49	20.6	10.2	6

4.2 Three-resistance two-capacitance model

Similar to the training method for the single capacitance model, training of the two-capacitance model was conducted with the constant exogenous heat supply assumption. It was found throughout the training procedure that meta-heuristic non-linear optimization algorithms, namely the Genetic Algorithm (GA) and the Particle Swarm Optimization (PSO) turned out to produce good results with a reasonable amount of computing resources in terms of training RMSE. Using the ode15s command in MATLAB, the solution for the training period was calculated from the continuous time space formulation discussed in the previous section with measured timeseries input data. For initial conditions, measured indoor temperature value at the start of the training period was used as the initial indoor air temperature, and the internal mass temperature was treated to be one of the parameters to be fitted during training procedure. The error between the predicted indoor temperatures from the solution and measured temperatures in hourly interval was calculated as RMSE, which was then accounted to be the cost function to be minimized with optimization algorithms. From the optimization routine, where the thermal parameters with initial internal mass temperature and unmeasurable exogenous heat supply are varied to reach the minimum RMSE, PSO and GA resulted in RMSE of 0.8981 ℃ and 1.2936 ℃ respectively during the training period. After evaluating each of the thermal parameters on their physical plausibility, it was decided that the fitting from PSO was to be used for the rest of the analysis. The thermal parameters obtained from the optimization are summarized in Table 2. The constant exogenous heat supply was 1.46 kW, and the initial internal mass temperature was 22.58 ℃ for this particular fit. One interesting observation is that there is quite a small amount of thermal resistance between the indoor air and the internal mass while their capacitance values are quite comparable. This makes the authors believe that in this formulation, the internal mass term behaves more like an additional zone in the building, providing an extra spatial dimension.

TABLE II. TRAINED PHYSICAL PARAMETERS OF 3R2C MODEL

Thermal Parameters						
A_m (m^2)	A (m^2)	R_{out} (*kW/°C*)	R_m (*kW/°C*)	$R_{m.out}$ (*kW/°C*)	C (*kWh/°C*)	C_m (*kWh/°C*)
5.89	1.21	3.23	0.64	10.99	9.50	9.98

As an effort to isolate the time-varying exogenous heat supply, a KF was used with the thermal parameters fitted above while treating the exogenous heat supply as a state without direct measurement, just like the internal mass temperature (Pergantis et al. 2024). While doing so, it was assumed that the exogenous heat supply had a static behavior. Therefore, the state space representation in discrete time for 3R2C model with exogenous heat supply as a state is expressed as below:

$$
\begin{aligned}
x_{aug}(k+1) &= \begin{bmatrix} [A_d] & [W_d] \\ [0\ 0] & 1 \end{bmatrix} x_{aug}(k) + \begin{bmatrix} [B_d] \\ [0\ 0\ 0] \end{bmatrix} u(k) + q(k) \\
y_{aug}(k+1) &= [\,1\ 0\ 0\,]\, x_{aug}(k) + v(k) \\
x_{aug} &= [\,T_{in}\ T_m\ Q_{exo}\,]^T
\end{aligned}
\tag{11}
$$

Here, the subscript, *d*, denotes the conversion of the matrices, *A*, *B*, and *W* discussed in previous section, from the continuous-time to the discrete-time formulation with sample time of 1 hour. The process noise *q(k)* is the disturbances to the system which are not accounted for even after the treatment of the exogenous heat supply as a system state variable. For modeling purposes, it was assumed that the process noise is an independent discrete noise, normally distributed around zero-mean, with variances of 0.01, 0.01, and 2 for the indoor temperature, internal mass temperature, and the exogenous heat supply, respectively. Likewise, the measurement noise, *v(k)*, was considered only for the one available measurement, indoor air temperature, where the uncertainty was assumed to be 0.1, considering the actual specification of the sensor used. These uncertainty values could be tuned for better performance of the KF, but intensive tuning effort was not spent as it was not the focus of this paper. The estimated exogenous heat supply by KF was then used as training data to build a prediction model discussed in the following section.

4.3 Exogenous thermal power training

Exogenous thermal power is the amount of heat which is generated or lost due to any factor except the HP. With limited data sets it is a challenge to get an estimate of exogenous power. Hence, many machine learning models were used initially to predict the response and the best out of these is selected for the main study. The time of the day, month, wind speed, outdoor temperature and solar irradiance are the input features of the model and exogenous power was the output feature. These are all leading causes of internal heat gains/losses, with the exception of the occupancy which was not recorded. However, this is captured to some extent in the time-of-day state. The model was trained for the four weeks in November with five cross fold validation to prevent overfitting.

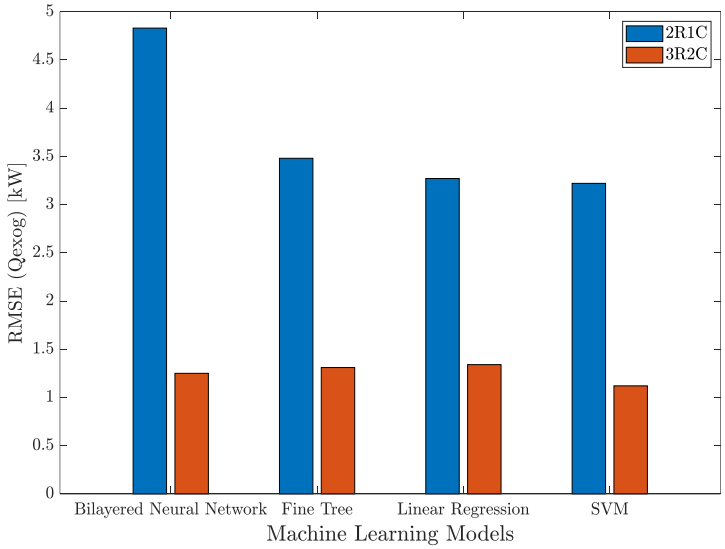

Figure 5: Variation of Exogenous Power with different input parameters.

The RMSE of different models that were considered is shown in Fig. 5. The same methodology was applied to the 2R1C and 3R2C models. The training datasets of 3R2C showed better results and amongst all the models, the SVM had the least error in the case of 2R1C and 3R2C which was 3.22 and 1.11 kW respectively, hence it was selected to forecast the future loads. Additionally, SVM is particularly efficient for small datasets (less than 1000). The higher RMSE of the 2R1C was due to the inherent larger magnitude of the exogenous heat supply since I_{solar} was not included explicitly in Eq. 1, without indicating a fit issue as validated by Fig. 7.The selected SVM model is tested against the new data sets from December 2022 to February 2023. The predicted exogenous thermal over these months is compared to RC fits and is shown in Fig. 6. The prediction error of the model was 3.88 and 3.56 kW for 2R1C and 3R2C respectively. The exogenous thermal power has varying spread in December and February while in January it is almost constant. This can be attributed to the setpoint adjustments, which are constant in January and varying in other months. The real physical dynamics of the house are both non-linear, and infinitely dimensional. By maintaining the indoor temperature constant, those additional DOFs are removed reducing the spread in the exogenous term. The spread in the latter and previous months is attributed to an hourly changing setpoint (smart control operation), resulting in unsteady dynamics.

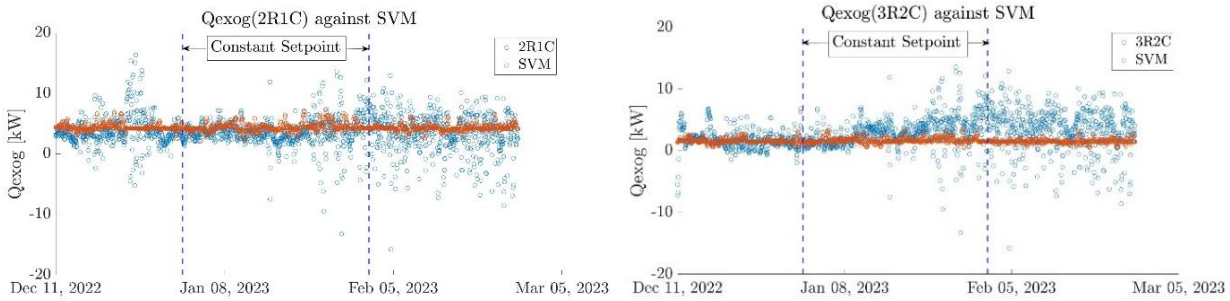

Figure 6: Variation of exogenous thermal power on test dataset.

5. EXPERIMENTAL VALIDATION

Having trained both the higher order (3R2C) and the lower order (2R1C) models, it is pertinent to compare their performance. The comparison of the two models in their prediction of the indoor air temperature is shown in Figure 8. A day ahead forecast was investigated, with the hidden state, Tm, being obtained using the Kalman filter described in Section 3C. It was found that the respective RMSE for 2R1C and 3R2C were 0.82 and 0.57 °C.

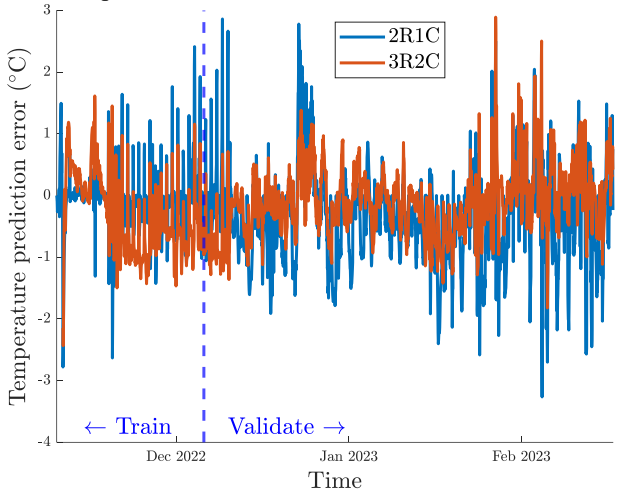

Figure 7: Step-ahead time series forecast error for the 2R1C model (blue) and 3R2C (orange). Both models show acceptable performance, although under the dynamic indoor conditions in February (RC model).

As expected, the higher dimensional model performance is better, although, the 2R1C model has an adequate RMSE, generally defined as less than 1 ℃ (Blum et al. 2019). With respect to the heat supply prediction, i.e., given a time series of temperatures, to predict what the input that went into the system was, for the 2R1C model this can be computed using Eq. 10, while for the 3R2C model (and any higher order nRyC model) by:

$$u(k) = \mathrm{B}^{\dagger}\left[x(k+1) - Ax(k) - Dd(k)\right] \tag{12}$$

where, $B^{\dagger}$ is the Moore-Penrose pseudo-inverse of the control input matrix B. Using these two expressions it is possible to find an RMSE of 2.4 kW for the heat supply prediction of the 2R1C model and 1.6 kW for the 3R2C model under transient indoor conditions. It should be noted that similar to the temperature, and steady indoor conditions, this difference is lesser.

Therefore, one should consider what are the comparative advantages and disadvantages of the two methods. One of the major disadvantages of higher order methods is the observability of the hidden states. This is tackled using a KF and utilizing the heat supply measurements from the house. However, the 2R1C only requires a temperature input to work. Therefore, the 3R2C method requires continuous monitoring of the heat supply (input state) making it an expensive solution for residential buildings. The 2R1C model on the other hand is much less expensive, since the sensors (electrical or thermal), could be installed for training purposes and then returned. Additionally, as validated from the 3R2C training results, the thermal mass closely followed the mixed air temperature, indicating fairly good thermal equilibrium. This indicates that the 2R1C model is an adequate solution for the DC House, although further testing in other detached residential buildings would further corroborate this.

6. CONCLUSIONS

This work presented a novel grey-box, resistance-capacitance model particularly suited for detached single family residential buildings, alongside an open-source tool-box for training RC models, something missing from the smart predictive controls community. The novelty rested in steering away from the state-of-the-art of using either black-box models which are particularly data intensive or high order grey box models, which though they offer slightly better performance require additional sensor costs making them in practical for real residential buildings. The low-order model was shown to have good prediction capabilities on a wide range of indoor and outdoor conditions. Future work will be directed in applying this methodology on a number of residential buildings across climates; currently only performed in a single cold-climate residential building, to further elucidate the appropriate model structure model for detached residential buildings.

NOMENCLATURE

C – Thermal Capacitance of air [kWh/℃]

R – Equivalent Thermal Resistance [kW/℃]

R_m – Thermal Resistance air-mass [kW/℃]

R_{out} – Thermal Resistance air-ambient [kW/℃]

θ – Ambient Temperature [℃]

θ_{eq} – Equivalent Ambient Temperature [℃]

$\dot{Q}_c$ – Thermal Power from HP + AUX [kW]

$\dot{Q}_e$ – Exogenous Heat Supply [kW]

T – Indoor Air Temperature [℃]

T_m – Envelope mass temperature [℃]

HP – Heat Pump

RMSE – Root Mean Square Error

LS – Least Squares

SVM – Support Vector Machine

AUX – Auxiliary Heat Electric Elements

REFERENCES

Energy Information Administration (EIA). Annual Energy Review 2021.
González-Torres, M., Pérez-Lombard, L., Coronel, J.F., Maestre, I.R., Yan, D. 2022. A review on buildings energy information: Trends, end-uses, fuels and drivers. Energy Reports 8: 626-637.
Drgona et al. 2020. All you need to know about model predictive control for buildings. Annual Reviews in Control 50: 190-232.
Zhang, K., Blum, D., Cheng, H., Paliaga, G., Wetter, M., & Granderson, J. 2022. Estimating ASHRAE guideline 36 energy savings for multi-zone variable air volume systems using spawn of EnergyPlus. Journal of Building Performance Simulation, 15(2): 215-236.
Dong, B., and Lam, K. P. 2013. A real-time model predictive control for building heating and cooling systems based on the occupancy behavior pattern detection and local weather forecasting. Building Simulation, 7(1).
Kim et al. 2022. Site demonstration and performance evaluation of MPC for a large chiller plant with TES for renewable energy integration and grid decarbonization. Applied Energy, 321.
Blum et al. 2019. Practical factors of envelope model setup and their effects on the performance of model predictive control for building heating, ventilating, and air conditioning systems. Applied Energy, 236, p. 410-425.
Coninck, D., R., Helsen, L. 2016. Practical implementation and evaluation of model predictive control for an office building in Brussels. Energy and Buildings 11: 290–298.
Pergantis, E. N., Reyes Premer, L., Lee, A. H., Priyadarshan, Liu, H., Groll, E. A., Ziviani, D., Kircher, K. J. (2024). Protecting residential electrical infrastructure through advanced control: The first field results, 8th International High Performance Buildings Conference. Paper 3138.
Pergantis, E. N., Priyadarshan, Theeb, N. A., Dhillon, P., Ore, J. P., Ziviani, D., Groll, E. A., Kircher, K. J. (2024). Field demonstration of predictive heating control for an all-electric house in a cold climate. Applied Energy, 360, 122820.
Khabbazi, A.J., Pergantis, E.N., Reyes Premer, L.D, Lee, A.H., Ma, J., Liu, H., Henze, G.P., Kircher, K.J. (2024). What Have We Learned From Field Demonstrations of Advanced Commercial HVAC Control? 8th International High Performance Buildings Conference. Paper 3503.
Pergantis, E. N., Reyes Premer, L., Priyadarshan, Lee, A. H., Dillhon, P., Ziviani, D., Groll, E. A., Kircher, K. J. (2024). Latent and sensible model predictive controller demonstration in a house during cooling operation. In: Proceedings of the ASHRAE Winter Conference.
Priyadarshan, E., Pergantis, C., Crozier, K., Baker, K., Kircher, K. J. (2024). Edgie: A simulation test-bed for investigating the impacts of building and vehicle electrification on distribution grids. In: Proceedings of the Hawaii International Conference on System Sciences.
Oikolab: Weather and Climate Data for Analysts, url: https://oikolab.com/
Grant, M., and Boyd, S. 2014. CVX Matlab Software for Disciplined Convex Programming, version 2.1. DOI: http://cvxr.com/cvx, March 2014.
U.S. Census Bureau. (2019). Characteristics of New Housing [Data file]. Retrieved from www.census.gov.
Pergantis 2024. A simpe Github repository for identifying building envelope gray-box models for detached residential buildings: https://github.com/epergant/Building-Identification-tool-box.git.

ACKNOWLEDGEMENTS

The Center for High-Performance Buildings (CHPB) at Purdue University supported this work (project CHPB-26-2023). E. Pergantis was also supported by the Onassis Foundation as one of its scholars, as well as the American Society of Heating and Refrigeration Engineers (ASHRAE) through a Grant-in-Aid award.